《報文》 HWAHAK KONGHAK Vol. 20, No. 5, October 1982, pp. 355—364
(Journal of the Korean Institute of Chemical Engineers)

루테늄 촉매표면에서의 화학흡착 및 촉매반응
——물의 흡탈착에 관한 연구——

이 호 인·이 문 득
서울대학교 공과대학 공업화학과

(1982년 6월 1일 접수)

Chemisorption and Catalysis on Well-Characterized Ruthenium Surfaces
——Adsorption and Desorption of Water——

Ho-In Lee and Moon-Deuk Lee
Department of Chemical Technology, College of Engineering,
Seoul National University, Seoul 151, Korea

(Received; June 1, 1982)

루테늄 촉매표면에서의 물의 흡탈착을 극초진공하에서 TDS, AES, LEED 등의 분석기술에 의하여 연구하였다. 물은 실온에서 분해가 되지 않은 분자형태로 흡착하여 1000분의 1 이하의 단분자 흡착층을 포화흡착량으로 가지며, 약 380 K에서 최대의 탈착속도를 나타낸다. 고온에서, 물은 표면에 흡착산소원자를 남기면서 분해하며, 약 480 K에서 최대분해속도를 나타낸다. 또한 분해된 표면산소원자의 촉매몸체속으로의 침투현상을 여러가지 방법의 실험으로 증명하였다.

ABSTRACT

The adsorption and desorption of water on the surfaces of ruthenium catalysts have been studied using the techniques of uptake, thermal desorption spectroscopy(TDS), Auger electron spectroscopy(AES), and low-energy electron diffraction(LEED) under ultrahigh vacuum conditions. Water adsorbs molecularly at room temperature giving a desorption peak at 380 K and a saturation coverage of less than a thousandth of a monolayer. At higher temperatures water dissociates leaving oxygen adatom, O(a), and the maximum dissociation rate is observed at 480 K. The dissociated surafce oxygen is evidenced to penetrate into the subsurface and/or the bulk.

1. Introduction

Ruthenium is one of the platinum group metals which are composed of the elements in group VIII of the fifth and sixth transition periods of the periodic table.

Recently, energy shortages are being seriously experienced in many parts of the world; consequently methanation processes are being studied vigorously in many laboratories. Early in the 1920's Fischer, Tropsch, and Delthey[1] compared the methanation properties of various metals at temperatures up to 800°C, and figured that the decreasing order of methanation activity was Ru, Ir, Rh, Ni, Co, Os, Pt, Fe, Mo, Pd, Ag. That is, ruthenium is recognized as a very active methanation catalyst; however, the high cost of this metal mitigated against its wide use. But when we consider long catalytic life, high activity and selectivity for the precious metal, ruthenium may be the best catalyst for methanation from oxides of carbon. There are only four metals which show a significant activity in the Fischer Tropsch synthesis. They are: iron, cobalt, nickel and ruthenium(nickel being somewhat less efficient than the other three). Ruthenium is the only one of these four metals which is used in the pure state, that is, unpromoted and unsupported. Iron requires promotion but not supporting, while cobalt and nickel are normally used with both promotors and supports, although unpromoted cobalt is highly active.

Problems of emission control from automobile exhaust are becoming serious for environmental conservation. Simultaneous catalytic control of three major pollutants in automobile exhaust, nitrogen oxides(NO_x), hydrocarbons (C_xH_y), and carbon monoxide(CO), requires both reduction of nitrogen oxides and oxidation of hydrocarbons and carbon monoxide. Most manufacturers of automobiles have used catalytic converters in their products since 1975. The term "three-way catalyst" is used to denote an ideal emission control catalyst which can eliminate the three major pollutant classes in automobile exhaust simultaneously. Ruthenium is known as the most effective catalyst(both very active and selective), in the absence of oxygen, for reducing NO to N_2 rather than NH_3 which is less environmentally desirable than N_2.[2-5] However, a major problem is the volatility of the higher ruthenium oxides.[2,6] The Ru-containing catalysts have poor stability under oxidizing conditions. Analysis of spent catalysts revealed severe losses of the active component, which were readily explained by the formation and removal of the volatile tetroxide.[2] Various studies were performed to minimize the tendency of the Ru to volatilize under oxidizing conditions while still preserving its high catalytic activity and selectivity. The incorporation of the basic oxide of barium made Ru(or its oxide) catalysts much more stable without losing high catalytic activity and selectivity.[7] Ruthenium is most effective as a three-way emission control catalyst when the air/fuel ratio is at near-stoichiometric values. Such ratios make for lower fuel economy, though.[8]

A fair number of studies of small molecule chemistry at well-define surfaces of ruthenium have been reported. In this study we will not discuss supported catalysts nor will we discuss high pressure studies. Rather, we will focus on low pressure studies on single crystal basal plane surfaces(001). As a part of a continuing series of surface studies involving Ru(001) and various adsorbates, we report here a study of the adsorption and

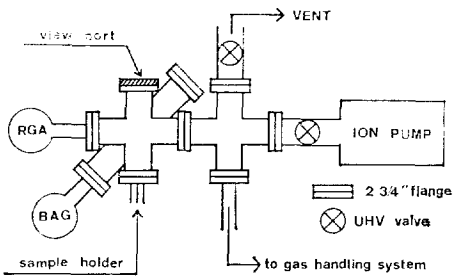

Fig. 1. Schematic diagram of the ultra-high vacuum system used in the TDS studies

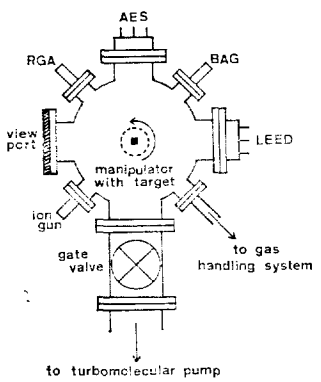

Fig. 2. Schematic diagram of the ultra-high vacuum system used in the AES/LEED studies

desorption of H_2O whose behaviors on the surface might affect strongly most of the reactions involving small molecules such as CO and H_2. That is, even though small in terms of species, energetics and concentrations (in the usual background pressures), water may give profound effetcs on catalytic rates and products. Our experiments rely on thermal desorption spectroscopy(TDS), low-energy electron diffraction(LEED) and Auger electron spectroscopy(AES).

2. Experimental

(1) Apparatus

The experiments were carried out in two different UHV systems. One was a small volume(1.35 *l*) system designed specifically for thermal desorption measurements and is shown schematically in *Fig. 1.* This ionpumped conductance-limited($S/V = 4$ sec^{-1}, where S and V represent the system pumping speed and volume, respectively) system had a base pressure in the 10^{-10} torr region but an operational base pressure of about 2×10^{-9} torr mainly CO and H_2 was characteristic during a series of measurements. The second system was a large turbomolecular-pumped chamber designed for AES and LEED measurements. A typical operational base pressure in this system was 1.5×10^{-10} torr which consisted mainly of H_2, CO and H_2O. A schematic diagram of this system is shown in *Fig. 2.*

(2) Substrate

The two substrates used in this project (one for each system) were cut from the same single crystal ruthenium rod supplied by the Materials Research Corporation, Orangeburg, New York. The nominal purity of this rod was 99.99%. The crystal was oriented using the Laue X-ray back scattering technique and cut by a standard electro-discharge spark cutting machine. The cut crystal discs were polished mechanically by the following step: (1) polish with a coarse emory cloth, (2) polish with a finer emory cloth, (3) polish with 0.3 micron alumina on a felt cloth adding ethanol to make suspension, (4) etch in boiling aqua regia for 2 hours, (5) take a Laue X-ray back scattering picture to identify a surface orientation desired. The Laue back scattering pattern indicated an orientation to within 1°of the (001) face, and the final thickness of the samples was 0.2 mm. The sample was mounted on three small tantalum leads 0.25 mm dia.) which were in turn connected to massive tungsten rods(2.5 mm dia.) covered

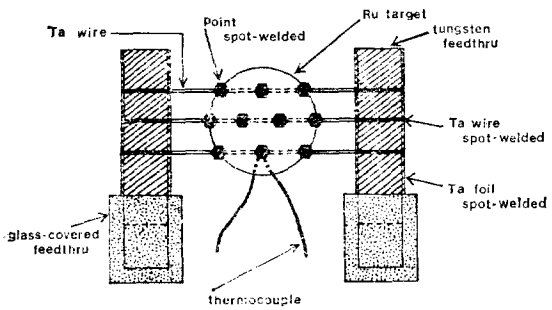

Fig. 3. Detailed diagram of the Ru-target

with uranium glass to reduce tungsten side effects especially when the target was heated to relatively high temperatures. The tungsten rods passed through the vacuum wall and served as heater leads. The target holder had two small nickel feedthrus for a thermocouple which was spot-welded on the back side of the target. *Figure 3* shows a detailed diagram of the target. The ten filled hexagonal points represent spot-welds of the target to the three tantalum leads. The ends of the tungsten rods were covered with a 0.025 mm-thick tantalum sheet, and the latter was spot-welded to the three small tantalum leads.

(3) Reagents

Water(H_2O and D_2O) was degassed at liquid nitrogen temperatures ten times(allowing the water to room temperature in each cycle). Water was introduced to the stainless storage tank as vapor at room temperature. All the reagents were introduced into the UHV chamber through variable leak valves from high pressure gas tank. The gas tank was refilled each day to minimize accumulated impurities. Occasionally the tank was baked out.

(4) Measurements

Temperatures of both the targets were measured with W-W 26% Re thermocouples with a diameter of 0.13 mm, which were spot-welded on the back-sides of the targets as shown in *Fig. 3*. The thermocouple wire was purchased from Omega Engineering, Inc., Stamford, Connecticut. Both the targets were heated resistively by using accurately resettable low-voltage, high-current ac supplies. Heating rates were changed slightly from one set of experiments to another but were typically 20-35 Ks^{-1}. In both systems, thermocouples were connected to 0°C reference junctions. The target temperatures could be controlled within ± 1 K in the range of 320 to 500 K as indicated by 6-digited voltmeters which could be read to the nearest microvolt. The uniformity of the target temperatures was checked in the range of 1000 to 1500 K by an optical pyrometer, and the temperature gradient across the target was not detectable(± 20K).

The total pressure was measured by an inverted ionization gauge, developed by Bayard and Alpert,[9] which measures over the range from 10^{-10} to 10^{-5} torr.

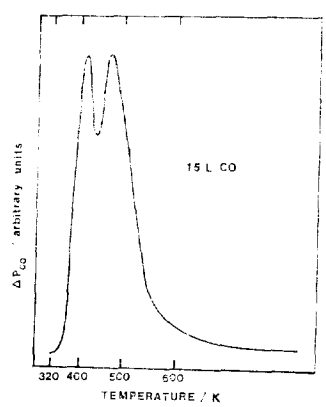

Fig. 4. Thermal desorption spectrum following adsorption of 15L CO on a clean Ru (001) at 320 K. Heating rate: 30 K/s

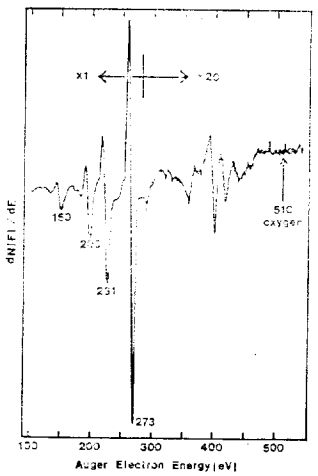

Fig. 5. Auger electron spectrum of clean Ru(001) following O_2 pretreatment for cleaning. Primary beam: 5 microamperes at 3.5keV, and modulation signal: 3eV(p-p)

3. Results and Discussion

(1) Cleaning samples

The samples were cleaned by heating for extended periods in 5×10^{-7} torr of O_2 at about 1500 K followed by periodic cooling and heating cycles at 1600-1700 K in vacuo. This oxygen treatment, vacuum heating-cooling cycle, had to be repeated many times in order to give a clean surface as judged either by the character of the CO desorption spectrum(usually by a saturated CO TDS spectrum) or by the AES spectrum. A 15 L CO TDS spectrum and an AES spectrum from a clean surface after the above oxygen pretreatment are shown in *Figs 4* and *5*, respectively. Typical impurities included O, C and S, and a tiny of Si was sometimes detected. Following this clean-up, the sample was annealed for a few hours in vacuo at 1300 K. Such a sample could usually be restored to a clean condition after a series of experiments by flashing briefly to 1700 K. Occasionally, however, the oxygen pretreatment, vacuum heating-cooling cycle, had to be repeated. The high temperature oxygen behavior was so complex and sometimes variable amounts(usually less than 5% of a monolayer) appeared which proved very difficult to remove. Along with this phenomenon, the penetration of surface oxygen into the subsurface or the bulk region made very slowly the surface catalytic behavior changed with a long, long-term use. The detailed results and discussion were published separately.[10]

(2) Chemisorption of water

A typical transient water mass spectrum

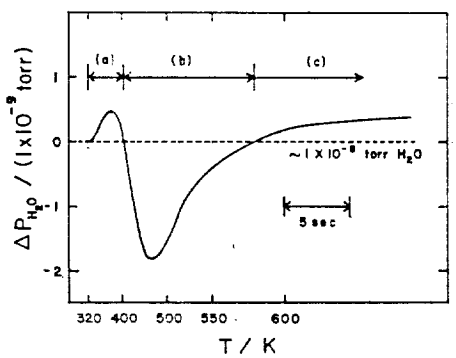

Fig. 6. A typical water desorption spectrum after a 10 L water exposure at 320 K. Region(a) (b), and (c) correspond to the regions of (a) desorption, (b) dissociation of water and interaction between H_2O and CO, and (c) side effects

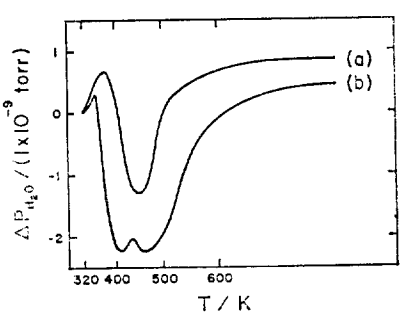

Fig. 7. H_2O TDS spectra under a constant leak of 1×10^{-8} torr of H_2O with (curve (b)) and without (curve (a)) a predosed 15 L CO at 320 K

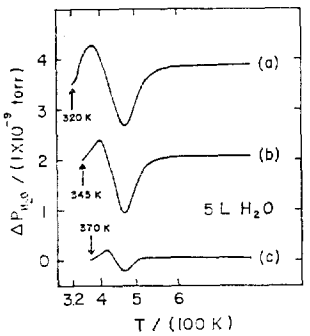

Fig. 8. H_2O TDS spectra following a 5 L H_2O exposure at three different temperatures: (a) 320 K, (b) 400 K, and (c) 490 K

produced by heating(30 Ks^{-1}) a surface exposed to 10 L H_2O(with 2×10^{-7} torr of pressure) at 320 K is shown in *Fig. 6*. At the beginning of the flash most of the back ground was water at about 1×10^{-8} torr due to its low pumping speed. This figure looks rather like a combined spectrum of desorption and uptake.

Although no room temperature adsorption data of H_2O on ruthenium surface are available, McCarty and Madix[11] have studied the adsorption of H_2O at 175 K on a clean Ni(110) surface and observed three different thermal desorption peaks, the highest temperature peak coming at 370 K. They are suggested that H_2O is molecularly adsorbed on this surface.

Region(a) of *Fig. 6* is suggested to be the region of an ordinary desorption of H_2O with a desorption peak at about 380 K. The area of this peak gives a saturation water coverage of less than 0.001 ML. We attribute this peak to the desorption of molecularly held water with reasons as follows: (1) Its area is dependent on the number of available adsorption sites at a constant temperature, i.e., the more available sites permit the bigger desorption area as seen in *Fig. 7*. (2) It also depends upon the adsorption temperature for a given exposure, i.e., lower temperature gives a bigger area as shown in *Fig. 8*. And (3) A large area occurs under a higher constant leak of H_2O at a constant temperature. This is also evidenced by an experiment which shows the same area regardless of the waiting intervals longer than one for saturation coverage under the same pressure of 1×10^{-8} torr H_2O.

Figure 7 shows two different H_2O TDS spectra under a constant leak of 1×10^{-8} torr of H_2O. Curves (a) and (b) correspond to the spectrum from a clean surface and from a surface predosed 15 L CO at 320 K, respectively. A decrease of the area of convex part of curve (b) and the shift of the peak position to lower temperature are observed. The relatively big differences of the concave parts between two spectra suggest a significant interaction between CO(a) and H_2O(a). The convex peak of curve (b) shifts to lower temperature presumably because of a repulsive interaction between the major CO(a) and the minor H_2O(a), and decreases peak height due to fewer available sites for adsorption because of the saturation of CO. A possible alternate explanation of the above is the adsorption of H_2O on the top of CO(a) molecules. The change of depth and shape of the concave peaks in *Fig. 7* will be discussed in more detail in terms of dissociation of water and interaction between CO and H_2O in a separate paper.[12]

In *Fig. 8* curves (a), (b), and (c) correspond to the H_2O TDS spectra following a 5 L H_2O exposure at 320 K, 400 K, and 490 K respectively. The results show that the area of the convex peak is strongly related to the adsorption temperature. Curves (a), (b), and (c) were flashed from 320 K, 345 K, and 370 K, respectively because the same cooling and

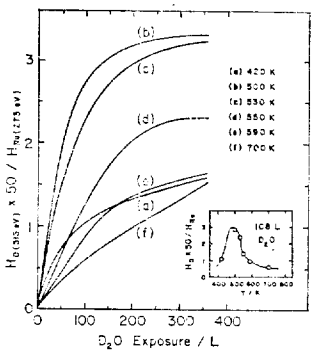

Fig. 9. Variations of the H_0/H_{Ru} as a function of D_2O exposure at six different fixed temperatures(where H_0 is the p-p height of oxygen Auger transition at 515 eV and H_{Ru} is that of ruthenium Auger transition at 273 eV). The inset shows the values of H_0/H_{Ru} at a fixed exposure of 108 L D_2O

evacuating times(5 min.) were used for comparison.

Region (b) of *Fig. 6* is suggested to be the dissociation of H_2O into hydrogen and oxygen on the surface. The maximum rate of dissociation and interaction with background CO occurs at about 470 K and results in a significant production of CO_2 and H_2. The reaction of H_2O with CO on the surface is proposed asfollows:

$$H_2O(a) \rightleftharpoons 2H(a) + O(a)$$
$$2H(a) \rightleftharpoons H_2(g)$$
$$CO(a) + O(a) \rightleftharpoons CO_2(g)$$

therefore, the overall reaction,

$$H_2O(a) + CO(a) \rightleftharpoons H_2(g) + CO_2(g)$$

is proposed. *Figure 9* shows that the maximum forward rate of the above first reaction occurs around 500 K which agrees well with the position of the concave peak of the region (b) in *Fig. 6*. This supports the idea that region (b) is properly designated as dissociative. The inset of *Fig. 9* further supports this proposal since it mirrors the shape of the (b) region of *Fig. 6*. Separate TDS experiments show the same result: For a 1L H_2O exposure, the oxygen desorption is larger by a factor of 4 if the water is exposed at 490 K rather than 400 K.

Figure 9 gives six curves for six different water adsorption temperatures. Each curve shows the variation of the H_0/H_{Ru}(where H_0 is the peak-to-peak height of oxygen Auger transition at 515 eV and H_{Ru} is that of ruthenium Auger transition at 273 eV) as a function of D_2O exposure at a fixed temperature. Clearly the value of H_0/H_{Ru} is sensitive to the adsorption temperature. The inset shows the behavior at an exposure of 108 L D_2O. The initial slope of H_0/H_{Ru} versus exposure gives a maximum around 500 K suggesting that D_2O is dissociated with a maximum rate at about 500 K. Curve (f) gives the smallest values of H_0/H_{Ru} throughout the exposure range studied but shows no sign of saturating like the curves at lower temperatures. That is, it shows a steady increase of H_0/H_{Ru} to the largest exposure used (360 L), unlike the other lower temperature curves. This suggests the penetration of surface oxygen into the bulk. This is supported by the results for O_2 uptake as a function of adsorption temperature presented elsewhere.[10] Comparing the results of O_2 and H_2O uptake obtained by AES, we find the adsorption rate of D_2O is smaller by a factor of about 100 than that of O_2 at 700 K(if all D_2O adsorbed is assumed to dissociate leaving O(a) on the surface). In a separate set of AES experiments where H_0/H_{Ru} was followed as a function of temperature for a 360 L D_2O exposure at several different adsorption temperatures, the same features are observed as in O_2 uptake experiments[10](except the big difference in rate as noted above) : i.e., (1) penetration of O(a) into the subsurface and/or the bulk, and (2)

Table 1. LEED Pattern as a Function of D_2O Exposure at Constant Temperatures

p_{D_2O} flowed = 6×10^{-8} torr

Exposure Time(sec)	100	150	200	250	300	350	400	500
Exposure(L)	6	9	12	15	18	21	24	30
LEED Pattern (w/ e^- beam, at 420 K)	(1 × 1)	(1 × 1)	(2 × 2)W*	(2 × 2)G*	(2 × 2)G	(2 × 2)E*	(2 × 2)E	(2 × 2)E
LEED Pattern (w/o e^- beam, at 380 K)	(1 × 1)	(1 × 1)	(1 × 1)	(2 × 2)W	(2 × 2)W	(2 × 2)G	(2 × 2)G	(2 × 2)E

* (2 × 2)W : Weak(2 × 2) LEED Pattern
(2 × 2)G : Good(2 × 2) LEED Pattern
(2 × 2)E : Excellent(2 × 2) LEED Pattern

Table 2. LEED Pattern as a Function of Temperature for Two Different Adsorption Temperatures and Exposures of D_2O

T_{ads} = 460 K, Exposure = 28.8 L

Temperature(K)	360	470	570	690	830	1070
LEED Pattern	(2 × 2)E	(2 × 2)E	(2 × 2)W	(2 × 2)W	(2 × 2)?	(1 × 1)

T_{ads} = 500 K, Exposure = 360 L

Temperature(K)	690	810	950	1080	1220	1350	1450
LEED Pattern	(2 × 2)E	(2 × 2)E	(2 × 2)G	2(× 2)G	(2 × 2)G	(2 × 2)G	(1 × 1)

shift of the desorption peak to lower temperature with higher adsorption temperatures.

In *Fig. 9* the crossing of curves (a), (d), and (e) are suggested to be due to the oxygen penetration into the bulk.[10] That is, in the initial stages, curve (a) grows more rapidly than curves (d) and (e) suggesting that less penetration occurs at 420 K than at 550 K and at 590 K. However, with increasing D_2O exposure, curves (d) and (e) exceed curve (a) suggesting that at higher temperatures the concentration builds up more rapidly in the near surface region sampled by AES. The earlier crossing of curve (d) with curve (a) than of curve (e) with curve (a) suggests that the dissociation rate of H_2O at 550 K is bigger than that at 590 K resulting in the faster saturation of subsurface region at 550 K. This agrees well with *Fig. 6* where the maximum rate of dissociation of H_2O occurs around 470 K.

The results of low-energy electron diffraction(LEED) studies are given in *Tables 1* and *2*. In *Table 1* changes of LEED pattern are shown as a function of D_2O exposure at two different fixed temperatures. *Table 2* shows LEED pattern changes as a function of temperature after adsorption of a given exposure of D_2O at a given temperature. Two very different exposures at about same temperature(460 K and 500 K) were used.

In the LEED study outlined in *Table 1*, if we assume no e^- beam effects on the LEED pattern, then it is evident that D_2O is more likely to dissociate at 420 K than at 380 K since the(2 × 2) oxygen pattern appears at lower exposure. This result is in good agreement with that from the TDS study. The maximum intensity of (2 × 2) O pattern appears at the exposure of about 1.5 L O_2,[13] so we can esti-

mate roughly the probability of D_2O dissociation at two temperatures, under the assumption of a negligible contribution of D_2O(a) to the(2 × 2) LEED pattern. Although the probability is expected to be lower when a dtectable oxygen impurity in D_2O is considered, we get values of about 0.05 and about 0.03 for the adsorption temperature of 420 K and 380 K, respectively. These values are uncertain by a factor of 2 due to the inaccurate determination of the maximum intensity of the LEED pattern.

The area of concave peaks in *Fig. 8* are related to the adsorption temperature of H_2O. Curve (c) with an adsorption temperature of 490 K has the smallest concave area suggesting that the surface has the least number of sites available for the dissociation of H_2O. This is apparently due to the occupation of sites by oxygen from dissociated H_2O during the exposure of a 5 L H_2O at 490 K. This strongly suggests that the dissociation of H_2O is maximized around 470 K. In addition, from *Fig. 8* we get two more features : (1) The dissociation rate of H_2O at 320 K is almost the same as that at 400 K which follows the explanation mentioned above. And (2) The temperature which gives a maximum dissociation rate of H_2O is independent of the H_2O adsorption temperature.

In another LEED study(*Table 2*), in the case of lower exposure(28.8 L D_2O), the (2 × 2) pattern begins to disappear at about 700 K which is much a lower temperature than that required for O_2 desorption. This suggests the easy penetration of surface oxygen into the subsurface or the bulk resulting in no detectable oxygen on the surface. On the other hand, in the case of higher exposure (360 L D_2O) we observe an excellent (2 × 2) and a good (2 × 2) LEED till 810 K and 1350 K, respectively. This suggests that oxygen penetrates significantly during a 360 L exposure at 500 K resulting in a high occupation of oxygen in the subsurface region. Since a relatively good (2 × 2) LEED persists even at 1350 K which is in the oxygen desorption region certain amount of segregation of subsurface oxygen to the surface is suggested in order to compensate the amount of desorption.

Region (c) of *Fig. 6* is assigned to side effects such as lead-wires by elevating temperature. The extent of the rise from the starting level increases with the final temperature of desoption or with holding time at a fixed final temperature.

4. Conclusion

(1) H_2O adsorbs molecularly on ruthenium at even room temperature giving a desorption peak at about 380 K and a saturation converage of less than a thousandth of a monolayer.

(2) The rate of dissociaiton of H_2O on Ru is very slow at room temperature and maximizes at about 470K. The products are mainly O(a) and H_2(g).

(3) The surface oxygen come from the dissociative adsorption of water is evidenced to penetrate into the subsurface and/or the bulk.

(4) Clean surface of the substrate is obtained by oxygen pretreatment at high temperatures over 1500 K, and the surface behavior of the substrate is very slowly changed due to the penetration of surface oxygen into the subsurface region.

Nomenclature

S pumping speed of the system

V system volume

UHV abbreviation for "ultra-high vacuum"

AES abbreviation for "Auger electron spectroscopy"

LEED abbreviation for "low-energy electron diffraction"

TDS abbreviation for "thermal desorption spectroscopy"

L langmuir(as a unit of exposure, equal to 1×10^{-6} torr·sec)

K unit of Kelvin temperature

s second(as a unit of time)

ML monolayer

$H(a)$, $H_2O(a)$, $CO(a)$, $O(a)$ adsorbed species considered

$H_2(g)$, $CO_2(g)$ gas-phase species considered

e^- electron

(2×2) one of LEED pattern proposed by Wood

H_0, H_{Ru} AES peak-to-peak height of strface species considered

Ru(001), *Ni*(110) Miller index for the plane of a single crystal considered

REFERENCES

1. F. Fischer, H. Tropsch and P. Dilthey, Brennstoff-Chem., 6 (1925) 265.
2. M. Shelef, Catal. Rev., 11(1975) 1.
3. James C. Schlatter and Kathleen C. Taylor, J. Catal., 49(1977) 42.
4. R.L. Klimisch and K.C. Taylor, Environ. Sci. Technol., 7(1973) 127.
5. T.P. Kobylinski and B.W. Taylor, J. Catal., 33(1974) 376.
6. W.E. Bell and M. Tagami, J. Phys. Chem., 67(1963) 2432.
7. M. Shelef and H.S. Gandhi, Plat. Met. Rev., 18(1974) 2.
8. Robert F. Gould(Editor), "Advances in Chemistry Series 143, Catalysts for the Control of Automotive Pollutants", American Chemical Society, Washington, D.C., 1975.
9. R.T. Bayard and D. Alpert, Rev. Sci. Instr., 21(1950) 571.
10. G. Praline, B.E. Koel, H.-I. Lee and J.M. White, Appl. Surface Sci., 5(1980) 296.
11. J.G. McCarty and R.J. Madix, Surface Sci., 54(1976) 121.
12. H.-I. Lee, to be published.
13. T.E. Madey, H.A. Engelhardt and D. Menzel, Surface Sci., 48(1975) 304.

Acknowledgements

The financial support from Ministry of Education of Korea is gratefully acknowledged and the authors thank Dr. J. M. White of the University of Texas, U.S.A. for valuable discussion and guidance to this work.